Specific heat and electrocaloric properties of $KTaO_3$ at low temperatures

W. N. Lawless
Research and Development Laboratory, Corning Glass Works, Corning, New York 14830
(Received 15 September 1976)

Specific-heat data (at zero field and 15.6 kV/cm), dielectric data, and electrocaloric data measured on a $KTaO_3$ crystal between 2 and 25 K are reported. The zero-field specific heat is about 30 times larger than the Debye prediction ($\Theta_D = 580$ K) at these temperatures but shows no anomaly characteristic of a sharp phase transition as suggested by the neutron data. A very broad transition is possible around 10 K for which $\Delta C = 0.11$ cal mol^{-1} K^{-1}. From the specific-heat difference C_0-C_E, a soft-mode frequency of 22.9 cm^{-1} is determined near 10 K. The electrocaloric effect consists of reversible and irreversible components. The reversible effect is in good thermodynamic agreement with the specific-heat and dielectric data and with published data on the Gibbs free-energy coefficients. Both the irreversible effect and the dielectric data indicate that $KTaO_3$ does not retain a center of symmetry at low temperatures.

I. INTRODUCTION

Low-lying vibrational modes in ferroelectrics have been extensively investigated by light and neutron scattering methods,[1] and recently published specific-heat data[2,3] on these materials have demonstrated that low-lying modes actually dominate the specific heat at low temperatures. As a general rule, any crystal structure that supports a soft mode, whether paraelectric, ferroelectric, or antiferroelectric, will have associated low-lying modes that contribute significantly to the low-temperature specific heat.[2]

Of all the ferroelectric materials, the cubic perovskite $KTaO_3$ (space group $Pm3m$) is perhaps the most attractive to study at low temperatures, for the following reasons: (i) $KTaO_3$ remains paraelectric down to the lowest temperatures so that complications resulting from domain-wall contributions to the specific heat[4] or from nonpolar transitions as in $SrTiO_3$ at 110 K are avoided; (ii) the elastic Debye temperature is large,[5] 580 K, so that low-lying modes will be emphasized at low temperatures (by contrast, the cubic paraelectrics PbF_2 and the thallous halides have Debye temperatures[2] ~ 100 K); and (iii) the soft-mode frequency is small, ~ 20 cm^{-1} at 10 K, well characterized by Raman,[6] dielectric,[7] and neutron[8] data, and is strongly field dependent.[6]

The purpose of this paper is to report for the first time specific-heat and electrocaloric measurements on an excellent single crystal of $KTaO_3$ in the temperature range 2–25 K. The soft mode in $KTaO_3$ should be manifested in the specific heat. Moreover, the neutron data have been interpreted[8] as indicating a nonpolar phase transition at 10 K, and evidence for such a transition should be seen in both the specific-heat and electrocaloric data. Finally, the electrocaloric data are not only a sensitive test of the Gibbs free-energy formalism, including the quantum-mechanical susceptibility, but also will indicate the attractiveness of $KTaO_3$ as a material for adiabatic-depolarization cooling (analogous to adiabatic demagnetization cooling in, say, cerium magnesium nitrate).

II. EXPERIMENTAL METHOD

The single crystal of $KTaO_3$, $0.701 \times 0.701 \times 0.122$ cm, was the same one measured by Samara and Morosin[7] and showed no strain birefringence at room temperature. All measurements here were made in the vacuum calorimeter described previously.[2] The crystal, outfitted with a machined radio-resistor thermometer (220 Ω, 1/8 W, 7 mg) and a 40-Ω manganin heater (3-Ω/cm, 0.04-mm-diam wire), was suspended inside an adiabatic shield on a 5-cm-long manganin wire (0.04 mm diameter). This wire was the thermal link and had a long time constant (~100 sec at 2 K). The major faces of the crystal were (100) faces and were electroded with a small amount of silver paste, and the voltage leads were attached with a spot of silver epoxy. All hookup leads were 0.025-mm-diam manganin wires which were thermally anchored to the adiabatic shield (a sapphire post was used to anchor the voltage leads). Portions (~1 cm) of the thermometer leads were tempered to the crystal. The addenda were determined by cumulative weighings (±0.2 mg) during sample assembly, and the addenda heat capacities as a percentage of the total heat capacity varied from 24 to 9% in the range 2–25 K, respectively. Literature data were used for the addenda corrections (see Ref. 2). A Fluke Model 408B Supply was the high-voltage supply, and the remaining experimental details are described in Ref. 2. It is believed that the specific-heat and electrocaloric measurements are accurate to ~ ±5%.

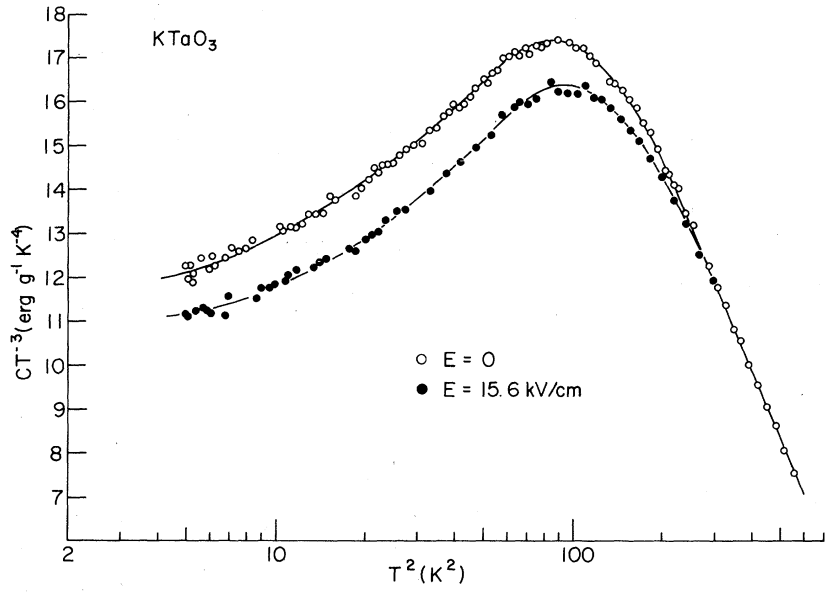

FIG. 1. Specific heat of $KTaO_3$ at zero field and at 15.6 kV/cm. There is little change in the position of the CT^{-3} maximum with applied field, and the specific heat is field independent above about 16 K.

III. EXPERIMENTAL RESULTS

A. Specific heat

Specific-heat data for $KTaO_3$ at $E=0$ and 15.6 kV/cm are shown in Fig. 1. The data are plotted as CT^{-3} to illustrate the non-Debye behavior: For $\Theta_D = 580$ K, $C_D T^{-3}$ = constant below about 25 K. Above about 16 K, the specific heat becomes field independent, and below 10 K the difference $C_0 - C_E$ is $\simeq 10\%$. The specific-heat data vary smoothly from 2 to 25 K and show no indication of a sharp phase transition at 10 K as has been suggested from neutron data[8] (see below, also).

The maxima in CT^{-3} shown in Fig. 1 suggest low-lying modes describable by Einstein terms, and the zero-field data can be adequately described by an Einstein term added to the Debye term.[2] However, such an analysis yields $\Theta_D = 182$ K, compared to the elastic-constant value[5] $\Theta_D = 580$ K. Therefore the Debye contribution to the specific is very small at these temperatures, $\simeq 3\%$.

The effect of an electric field is to reduce the specific heat as seen in Fig. 1, indicating field-dependent phonons. Further, it is known from Raman data[6] that the soft mode at ≈ 22 cm^{-1} ($E=0$) is shifted to ≈ 57 cm^{-1} at $E \simeq 16$ kV/cm. Experimentally, it was found here that the difference $C_0 - C_E$ appears to saturate for field strengths ~15

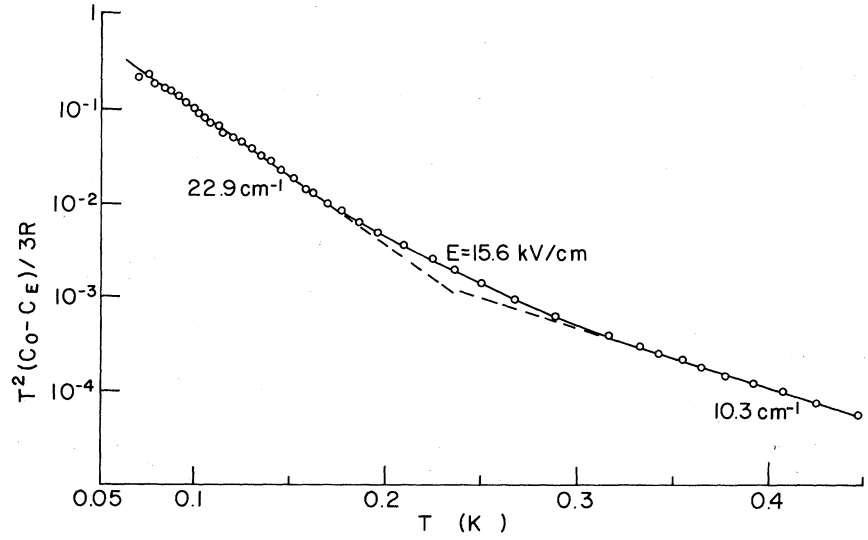

FIG. 2. Einstein plot of the specific-heat difference $C_0 - C_E$. The 22.9-cm^{-1} mode is the soft-mode frequency at $E=0$ (see text).

kV/cm, which implies that the difference $C_0 - C_E$ involves only *field-dependent* phonons. This means that the field-dependent phonons contributing to C_0 are sufficiently hardened by the $E = 15.6$ kV/cm field that their contribution to C_E is negligible in the temperature range of interest (see below).

Expressing the specific-heat difference as an Einstein term

$$C_0 - C_E = 3rRx^2e^x(e^x - 1)^{-2} \quad (1)$$

means that the slopes of an Einstein plot of $C_0 - C_E$ are related to the frequencies of the field-dependent modes, and this plot is shown in Fig. 2. These data were generated from the smoothed data of Fig. 1, and the difference $C_0 - C_E$ is independent of the Debye temperature and of the large density of field-independent phonons.

Two field-dependent phonons are indicated in Fig. 2, $\omega = 22.9$ and 10.3 cm^{-1}. The former is most probably the soft mode (at $E = 0$), and this frequency agrees well with the soft-mode frequency in $KTaO_3$ reported by Samara and Morosin[7] from dielectric data, $\omega_s = 22.3$ cm^{-1} at 10 K. The 10-cm^{-1} mode in Fig. 2 at the lower temperatures is probably not an impurity mode because the specific-heat contribution from a dipolar impurity will increase, rather than decrease, with an electric field.[9] This mode may be due to the low-energy TA phonons revealed by the neutron data[8] below 16 cm^{-1} and sufficiently coupled to the soft mode to be hardened by the electric field.

Returning to the assumption above, the 22.9 → 57 cm^{-1} shift of the soft mode by $E \simeq 16$ kV/cm implies that the ratio of the corresponding Einstein terms for this mode at $E = 16$ kV/cm and $E = 0$ varies from 0.5 to 5% over the T^{-1} range in Fig. 2. Therefore, the assumption that the soft-mode contribution to C_E is negligible in the temperature range of interest appears valid.

The large discrepancy between the measured specific heat and the Debye contribution for $\Theta_D = 580$ K appears due to field-independent phenomena. A possible explanation here may be a broad phase transition around 10 K, analogous to the field-independent phase transition in $SrTiO_3$ at 110 K. Such a phase transition in $KTaO_3$ has been proposed[8]. Noticeable line broadening of the soft mode was observed at 4 K, and for the TA modes at $q = 0.25$ and 0.30 $Å^{-1}$, a pronounced anomaly was seen at 10 K in the Bragg reflection. Around 10 K, the soft mode between $q = 0.1$ and 0.2 is degenerate with the corresponding LA mode, and the argument put forth here is by way of analogy with $SrTiO_3$, where a similar degeneracy coincides with the 110 K transition.[10]

Such a phase transition in $KTaO_3$ would have to be very broad because the CT^{-3} plot will emphasize a sharp transition. If a phase transition is invoked, the Fig. 1 data yield $\Delta C \cong 0.11$ cal mol^{-1} K^{-1} at 10 K using $\Theta_D = 580$ K. This value for the excess specific heat agrees remarkably well with the corresponding value for $SrTiO_3$,[11] $\Delta C = 0.10$ cal $mol^{-1}K^{-1}$. In $SrTiO_3$ the specific heat varies continuously within a 2-K-wide transition region.[11]

B. Electrocaloric data

An electrocaloric measurement consists of measuring the temperature change following a voltage change and so is very similar to a specific-heat measurement. The addenda corrections enter as

$$\Delta T_{\text{cryst}} = \Delta T_{\text{meas}}(1 + C_a/C_c),$$

where C_a and C_c are the heat capacities of the addenda and crystal, respectively. The Fig. 1 data for $KTaO_3$ were used in making this correction, and the field dependence of C_c was approximated by a linear correction (although not reported here, C_E varies approximately linearly with E up to saturation at about 15 kV/cm, as mentioned above—the effect, however, is not large, $C_E/C_0 \geq 92\%$ for $E \leq 15.6$ kV/cm).

A typical chart trace of a set of electrocaloric measurements is shown in the photograph, Fig. 3. The electrocaloric effect is not reversible as the ΔT on polarization heating ($0 \rightarrow E$) is larger in magnitude than the ΔT on depolarization cooling ($E \rightarrow 0$). At the lowest temperatures, heating was observed on *both* field changes, whereas at the highest temperatures the effect approaches reversibility.

In analyzing these data, it was assumed that the temperature changes ΔT consisted of a reversible component ΔT_e, and an irreversible or hysteretic component ΔT_h. The sign of ΔT_e depends on the sign of the field change, whereas the sign of ΔT_h does not, and from the cycle $0 \rightarrow E \rightarrow 0$ both components could be determined. Electrocaloric data are shown in Fig. 4, where the open symbols

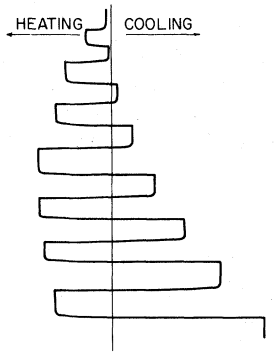

FIG. 3. Chart trace of a typical set of electrocaloric measurements with heating ($0 \rightarrow E$) and cooling ($E \rightarrow 0$) as indicated. Note the gradual drift of the center line to a higher temperature, indicative of the irreversible hysteretic heating component.

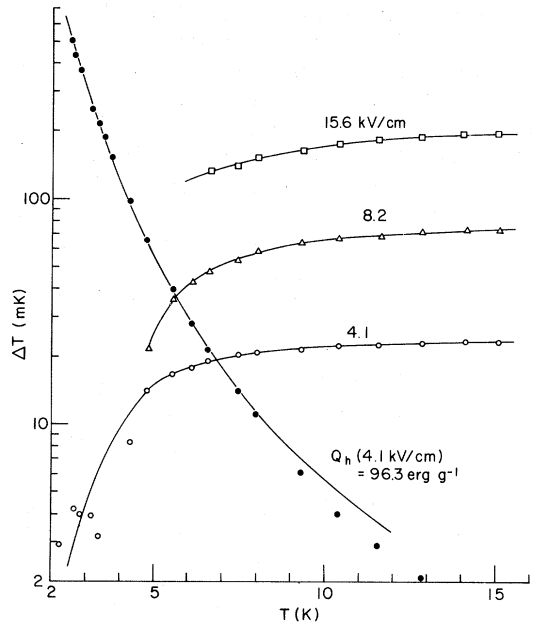

FIG. 4. Reversible electrocaloric component (open symbols) and irreversible component (full circles) of the temperature changes observed. The solid curve through the irreversible component at 4.1 kV/cm was scaled from the specific-heat data in Fig. 1, using $Q_h = 96.3$ erg g^{-1} according to Eq. (2). Note that at this field strength, no cooling effects were observed below about 7 K.

are the reversible components at three field strengths and the solid circles are the hysteretic components at 4.1 kV/cm. For example, at this field strength, actual cooling effects are observed only *above* 7 K, the $\Delta T_e - \Delta T_h$ crossover temperature.

The curve through the ΔT_h points in Fig. 4 at 4.1 kV/cm was drawn using the specific-heat data of Fig. 1 and a (fitted) $Q_h = 96.3$ erg g^{-1} according to

$$Q_h = C\Delta T_h \,. \tag{2}$$

The scaling of the specific-heat and ΔT_h data over several orders of magnitude is evidence that hysteretic heating occurs in $KTaO_3$ at these temperatures and that the hysteresis is approximately *temperature independent*. A similar scaling was observed at all field strengths, and in Fig. 5 are shown the Q_h data generated from the ΔT_h data, according to Eq. (2) and plotted versus E^2. As expected for hysteretic heating, $Q_h \propto E^2$ for small field strengths, and saturation effects set in at the higher field strengths.

The hysteresis in P-E was measured at 1.9 and 10 K by measuring $\epsilon(E)$ at 1 kHz on increasing and decreasing field strength and numerically integrating

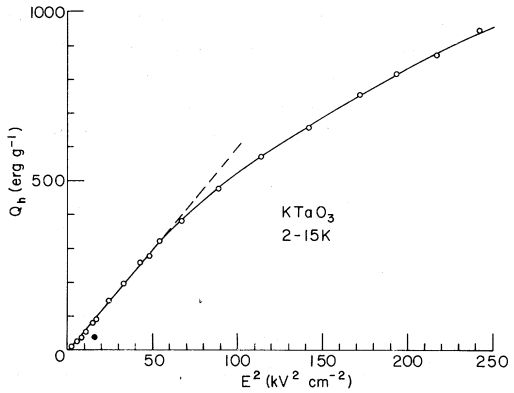

FIG. 5. The variation of the hysteretic heating Q_h with E^2. The Q_h values are temperature independent in the temperature range of interest. The solid circle at 4 kV/cm is the hysteretic heating calculated from 1 kHz dielectric measurements (see text).

$$P(E) = \int_0^E \epsilon(E')\, dE' \,. \tag{3}$$

Loop openings were observed at both temperatures. Hysteretic heating was calculated from

$$Q_h = \tfrac{1}{2} \oint P\, dE, \tag{4}$$

and in Fig. 5 the solid circle at 4.1 kV/cm ($\simeq 40$ erg g^{-1}) is the result of this calculation at 1.9 K. The agreement is satisfactory given the different experimental conditions. [Strictly speaking, Eq. (4) is the energy dissipated in traversing the loop slowly under isothermal conditions, whereas the electrocaloric hysteresis corresponds to the energy dissipated adiabatically following a very rapid field change.]

The reversible component ΔT_e is described thermodynamically by the $T\,dS$ relation[9]

$$T\,dS = C_E\, dT + T\left(\frac{\partial P}{\partial T}\right)_E dE \,. \tag{5}$$

The temperature changes are measured under adiabatic conditions ($dS = 0$), and because of the relatively small temperature changes involved, we have from Eq. (5)

$$\frac{C_E}{T}\Delta T_e = -\int_0^E \frac{\partial P}{\partial T}\, dE' \tag{6}$$

for the reversible polarization heating. For depolarization cooling, the limits of the integral are reversed.

The temperature derivative $(\partial P/\partial T)_E$ is evaluated according to the usual Gibbs free-energy function[11,12]

$$A = A_0 + \tfrac{1}{2}\chi P^2 + \tfrac{1}{4}\xi P^4 + \zeta \tfrac{1}{6} P^6 \tag{7}$$

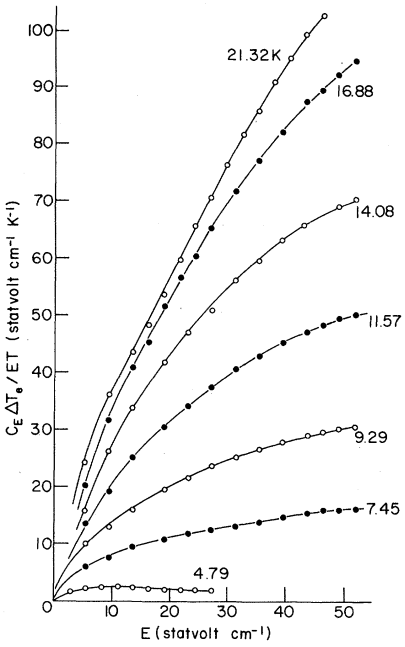

FIG. 6. Electrocaloric data on $KTaO_3$ plotted according to Eq. (8). The specific-heat data of Fig. 1 were used to construct the plot, and the temperatures indicated are average temperatures for the data sets.

for a centrosymmetric crystal where E and P are along [100]. From Eq. (7), $E=(\partial A/\partial P)_T$ and $\chi=(\partial^2 A/\partial P^2)_T=4\pi/\epsilon$, the reciprocal dielectric suspectibility. Performing the indicated operations we find from Eq. (6) that

$$C_E \Delta T_e / T E = aE + bE^3 + cE^5 , \tag{8}$$

where

$$a=\tfrac{1}{2}\chi'/\chi^2, \quad b=-\xi\chi'/\chi^5,$$
$$c=21\xi^2\chi'/6\chi^8-\zeta\chi'/\chi^7 . \tag{9}$$

In arriving at Eq. (9), ξ and ζ are assumed temperature independent, and $\chi'=d\chi/dT$.

We note from Eqs. (8) and (9) that $\Delta T_e \propto \chi' \propto d\epsilon/dT$. Therefore, from the dielectric data shown in Fig. 8 below, we expect ΔT_e to decrease rapidly below about 5 K. The Fig. 4 data are seen to agree qualitatively with this, and this lends additional confidence to the separation of the hysteretic and reversible components discussed above.

In Fig. 6 are shown sets of electrocaloric data plotted according to Eq. (8) versus field strength E for seven temperatures between 4.8 and 21.3 K. Data at the lowest temperature were limited to smaller field strengths because of the hysteretic heating, and more electrocaloric data were measured than are shown in Fig. 6. The parametric temperatures given in Fig. 6 are average temperatures, and the experiments were conducted such that the average temperature was maintained to $\lesssim \pm 1\%$ for all field strengths. The specific-heat data C_E used to construct the Fig. 6 plots were taken from Fig. 1 using the linear interpolation between C_0 and C_E discussed previously.

The Fig. 6 data were fitted to Eq. (8) using multiple regression methods, and the resulting coefficients of Eq. (7) calculated from Eqs. (9) are shown plotted in Fig. 7 versus temperature. The multiple correlation coefficients for these fits to Eq. (8) were $\gtrsim 0.9$, except for the 4.79- and 21.32-K data sets for which the correlation coefficients were $\simeq 0.8$.

The linear coefficient of the electrocaloric data is related to the dielectric constant by $\chi'/\chi^2 = -4\pi\, d\epsilon/dT$. To make this comparison, the dielectric constant of the $KTaO_3$ crystal was measured between 2 and 25 K (1 kHz) and these data are shown in Fig. 8. These data were fitted to the quantum-mechanical model of Barrett[13]

$$\epsilon = B[(T_1/2)\coth(T_1/2T) - T_0]^{-1}, \tag{10}$$

resulting in $B=6.18\times10^4$, $T_1=48.28$ K, and $T_0=8.02$ K.[14] The solid curve in the χ'/χ^2 plot of Fig. 7 was drawn using these fitting parameters in Eq. (10). The agreement is quite satisfactory between the dielectric and electrocaloric χ'/χ^2 data, espec-

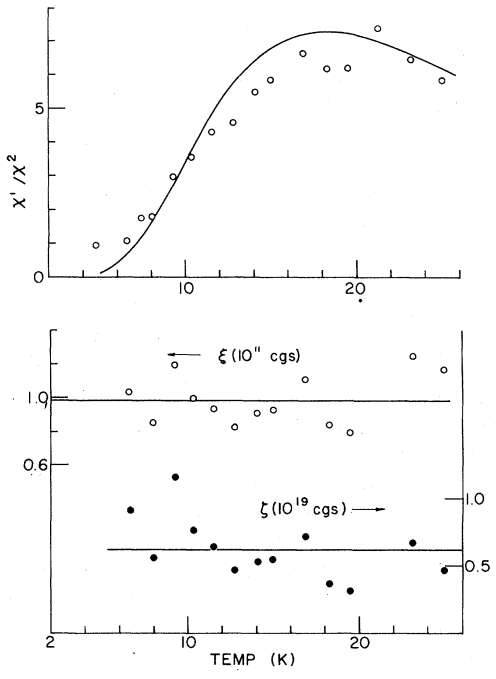

FIG. 7. Temperature variation of the coefficients χ'/χ^2, ξ, and ζ, as determined from fitting the Fig. 6 data to Eq. (8). The solid curve in the χ'/χ^2 plot is derived from the Fig. 8 dielectric data, using Eq. (10). Average values for the ξ and ζ coefficients are shown.

ially as χ and χ', according to Eq. (10), are sensitive to T_1 and T_0 in this temperature range.

The constants ξ and ζ describe the nonlinear response of the crystal. For $\xi > 0$, as in Fig. 8, the phase transition in $KTaO_3$ would be second order, if it were to occur. The data in the lower plots of Fig. 7 indicate that the fourth-order coefficient ξ is constant in this temperature range and equal to 0.98×10^{-11} (cgs), the average value shown. A negative temperature coefficient for the sixth-order coefficient ζ is suggested in Fig. 7, but this may not be real because of the experimental uncertainties. That is, at the lower temperatures, the separation of the reversible and irreversible components introduces an uncertainty in ΔT_e, whereas at the higher temperatures, the combined effects of increased specific heat and reduced thermometer sensitivity introduce uncertainty in ΔT_e. Consequently, the average value is shown in Fig. 7, $\zeta = 0.62 \times 10^{-19}$ (cgs).

These average values for ξ and ζ from the electrocaloric data agree quite well with published data: From field-induced Raman scattering data at 10 K, Fleury and Worlock[6] report 1.2×10^{-11} and 0.60×10^{-19}(cgs), respectively (1.0×10^{10} and 4×10^{12} in mks units). Kahng and Wemple report $\xi = 1.1 \times 10^{11}$ (cgs) for $KTaO_3$ at 4 K from nonlinear dielectric data.[14,15]

IV. DISCUSSION

A rather large amount of new data on the specific-heat and electrocaloric properties of $KTaO_3$ between 2 and 25 K have been measured, and it has been found that the specific-heat data (Fig. 1) and electrocaloric data (Fig. 6) are consistent with the thermodynamic description, Eq. (5), and with the dielectric data (Fig. 8), according to the quantum-mechanical model, Eq. (10). Moreover, the Gibbs free-energy expansion, Eq. (7), adequately describes the nonlinear response of the crystal, and the expansion coefficients determined from the electrocaloric data agree well with published values for these coefficients.

The specific heat of $KTaO_3$ is not as straightforward as had been originally anticipated based on the 580 K Debye temperature. Either a large density of acoustic phonons around 30 cm^{-1} or a very broad phase transition has to be invoked to explain the factor of 30 between the measured and the Debye specific heats. For the latter, the excess specific heat is tantalizingly close to the corresponding value for $SrTiO_3$. On the other hand, one would expect a phase transition to be particularly evident in a CT^{-3} plot (Fig. 1).

A definitive experiment here would be the optical observation of twinning in $KTaO_3$, as has been observed in $SrTiO_3$ below 110 K.[16] Along this line,

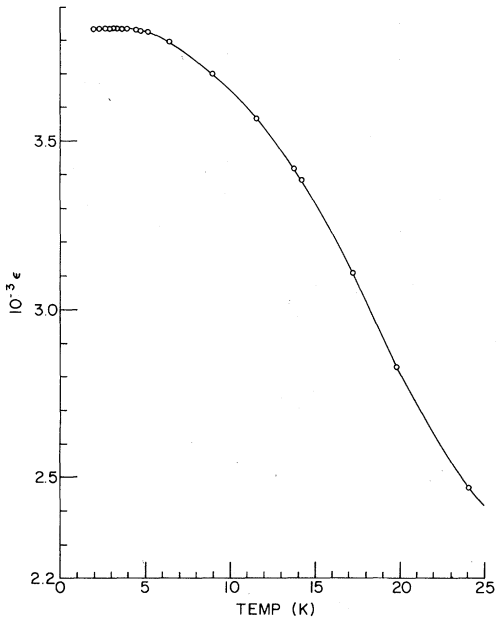

FIG. 8. Dielectric constant data at 1 kHz, measured on the same crystal used in the specific-heat and electrocaloric measurements.

Axe *et al.*[17] have investigated the quasiharmonic coupling of TO-TA phonons in relation to $KTaO_3$ and have suggested that the lattice might first become unstable with respect to an acoustic phonon with nonzero wave vector *before* the $q = 0$ optic mode goes to zero, leading to a microtwinned ferroelectric state.

The presence of the hysteretic component in the electrocaloric measurements and the loop openings observed in the dielectric data indicate that $KTaO_3$ does not retain a center of symmetry at these low temperatures. A similar conclusion was reached by Geusic *et al.*,[18] who reported that the nonlinear dielectric properties of $KTaO_3$ at 4 K could not be explained if a center of symmetry existed.

The soft-mode frequency determined from the $C_0 - C_E$ difference, 22.9 cm^{-1}, is in very good agreement with published values of this frequency at low temperatures.

ACKNOWLEDGMENTS

I am indebted to Dr. G. A. Samara for generously loaning the excellent $KTaO_3$ single crystal and for several stimulating discussions. The hospitality of the Cryogenics Division, U. S. Natl. Bur. Stand., Boulder, Colo., where these measurements were performed, is gratefully acknowledged. Assistance with computer processing by B. Bender at U. S. Natl. Bur. Stand., Boulder, Colo. and by Dr. D. Davis at Corning Glass Works is gratefully acknowledged.

[1]J. F. Scott, Rev. Mod. Phys. 46, 83 (1974); R. Blinc and B. Zeks, *Soft Modes in Ferroelectrics and Antiferroelectrics* (American Elsevier, New York, 1974).
[2]W. N. Lawless, Phys. Rev. B 14, 134 (1976).
[3]W. N. Lawless, Ferroelectrics (to be published).
[4]W. N. Lawless, Phys. Rev. Lett. 36, 478 (1976).
[5]Measured by R. Reed and H. Leadbetter (U.S. Natl. Bur. Stand., Colo.) on the same crystal (private communication).
[6]P. A. Fleury and J. M. Worlock, Phys. Rev. 174, 613 (1968).
[7]G. A. Samara and B. Morosin, Phys. Rev. B 8, 1256 (1973).
[8]G. Shirane, R. Nathans, and V. J. Minkiewicz, Phys. Rev. 157, 396 (1967).
[9]W. N. Lawless, J. Phys. Chem. Solids 30, 1161 (1969).
[10]R. A. Cowley, Phys. Rev. 134, A981 (1964).
[11]P. R. Garnier, Physics Lett. A 35, 413 (1971).
[12]See F. Jona and G. Shirane, *Ferroelectric Crystals* (MacMillan, New York, 1962), Chap. 1.
[13]J. H. Barrett, Phys. Rev. 86, 118 (1952).
[14]Samara and Morosin, Ref. 7, give slightly different values for these parameters, but their fitted data extend to room temperature.
[15]D. Kahng and S. H. Wemple, J. Appl. Phys. 36, 2925 (1965).
[16]E. Sawaguchi, A. Kikuchi, and Y. Kodera, J. Phys. Soc. Jpn. 18, 459 (1963).
[17]J. D. Axe, J. Harada, and G. Shirane, Phys. Rev. B 1, 1227 (1970).
[18]J. E. Geusic, S. K. Kurtz, T. J. Nelson, and S. H. Wemple, Appl. Phys. Lett. 2, 185 (1963).